Contents lists available at Science-Gate

International Journal of Advanced and Applied Sciences

Journal homepage: http://www.science-gate.com/IJAAS.html

Aligned magnetohydrodynamic effect on magnetic nanoparticle with different base fluids past a moving inclined plate

Fazillah Bosli [1], Mohd Rijal Ilias [2,*], Noor Hafizah Zainal Aznam [1], Siti Shuhada Ishak [2], Shahida Farhan Zakaria [1], Amirah Hazwani Abdul Rahim [1]

[1]*Mathematical Sciences Studies, College of Computing, Informatics and Media, Universiti Teknologi MARA (UiTM) Kedah Branch, Sungai Petani Campus, 08400 Merbok, Kedah Darulaman, Malaysia*
[2]*School of Mathematical Sciences, College of Computing, Informatics and Media, Universiti Teknologi MARA, 40450 Shah Alam, Selangor, Malaysia*

ARTICLE INFO

Article history:
Received 26 July 2021
Received in revised form
12 September 2022
Accepted 14 December 2022

Keywords:
Aligned MHD
Convective boundary condition
Free convection
Magnetic nanofluids
Moving inclined plate

ABSTRACT

This paper deals with the numerical solutions for the aligned MHD free convection laminar boundary layer flow over a moving inclined plate for two magnetic nanofluids, namely Fe_3O_4-water and Fe_3O_4-kerosene. It is assumed that the left surface of the plate is in contact with a hot fluid while the cold fluid is on the right surface. The mathematical model has been constructed and based on the Tiwari-Das model, appropriate similarity transformations are used to convert the governing partial differential equations into nonlinear ordinary differential equations and solved numerically using the Keller-Box method. Numerical results for the skin friction coefficient and local Nusselt number were presented whilst the velocity and temperature profiles were illustrated graphically and analyzed. It is found that the velocity increases and temperature decrease with an increase of aligned magnetic field angle parameter, magnetic strength parameter, and Grashof number while the velocity decreases and temperature increase when inclined plate angle parameter and volume fractions of nanoparticles increase. For the convective parameter, both velocity and temperature profile increase when the Biot number increase. Comparisons with previously published studies are performed and excellent agreement is obtained.

1. Introduction

Nanofluids have wide applications in various fields and have provided significant importance towards the enhancement of heat transfer. Their applications include desalination, cavity problem, solar thermal collector, nuclear system cooling, electronics cooling, solar water heating, heat exchanger, biomedicine, fuel cells, transportation (engine cooling/vehicle thermal management), and so on (Wu and Zhao, 2013; Hussein et al., 2014; Mitra, 2018). The term 'nanofluids' refers to a new class of engineered heat transfer fluids, which contain metallic particles with average particle sizes of 10nm and can be produced by current nanophase technology. The term was initially introduced by Choi and Eastman (1995).

Magnetic nanofluids consist of a colloidal mixture of magnetic nanoparticles with sizes in the range of 2–10nm and base liquid (Philip et al., 2007). The magnetic features of magnetic nanofluids are comparable to those of bulk magnetic materials and allow the retaining of common Newtonian fluids' flow characteristics. As indicated by several studies, a variety of techniques is applied to enhance heat transfer processes, especially for several ordinary fluids including water, toluene, ethylene glycol, and mineral oils. An innovative way to improve the heat transfer performance of fluids is to suspend nanophase particles in heating or cooling fluids (Xuan and Li, 2000; Alsaedi et al., 2012). Kamal et al. (2019) concentrated on the conjugate study of flow and heat transfer considering two physical effects such as g-jitter and thermal radiation on a three-dimensional stagnation point region. Recently, Nayan et al. (2022) used hybrid nanofluids in their study to increase heat transfer performance.

Magnetohydrodynamic (MHD) deals with the study of electrically conducting fluids that can move around in a magnetic field. An electric current is induced in the fluid when there is a change in the

* Corresponding Author.
Email Address: mrijal@uitm.edu.my (M. R. Ilias)
https://doi.org/10.21833/ijaas.2023.03.013
Corresponding author's ORCID profile:
https://orcid.org/0000-0001-6226-2389

magnetic field that cuts the moving fluid. Rana et al. (2012) investigated an incompressible nanofluid's steady mixed convection boundary layer flow along an inclined plate that was embedded in a porous medium. In their study, it was observed that the Nusselt number decreased with a rise in the thermophoresis number or Brownian motion number, whereas increasing the plate's angle led to an increase in the Nusselt number. Research by Ilias et al. (2017) focused on the free convection boundary layer flow over an inclined plate for two ferrofluids, Fe_3O_4-water and Fe_3O_4-kerosene. The numerical solutions are carried out by the Keller-Box method. It can be concluded that the skin friction and heat transfer rate of both ferrofluids are increasing in all parameters except for the angle of the inclined plate. Anjali Devi and Suriyakumar (2013) examined the numerical solution of MHD mixed convection nanofluid flow over an inclined stretching plate by considering the heat generation and suction effects. Mohamad et al. (2017) conducted a study to investigate the unsteady MHD boundary layer flow of a Casson fluid in a porous medium past an arbitrary wall shear stress vertical plate with mass and heat transfer. Meanwhile, Noranuar et al. (2021a; 2021b) used two types of carbon nanotubes which are single-walled carbon nanotubes and multi-walled carbon nanotubes in non-coaxial rotation flow affected by magnetohydrodynamics and porosity to analyze the fluid flow and heat transfer. In recent years, numerous authors have investigated the issues associated with the MHD boundary layer flows and heat transfer by considering the different problems and situations (Sheikholeslami and Ganji, 2014; Reddy et al., 2017; Ullah et al., 2017; Ilias et al., 2018; 2020; Ahmad et al., 2019; Ismail et al., 2021; Bosli et al., 2022).

Many industrial applications, natural processes, and chemical processing systems are faced with free convection processes that involve a combination mechanism of mass and heat transfer. The convective boundary condition is mostly used to define a linear convective heat exchange condition for one or more algebraic entities in thermal. Ostrach (1952) who started the convection flow study, used an integral method to make a technical note on transient free convection flow's similarity solution past a semi-infinite vertical plate. Rawi et al. (2016; 2018) studied the effect of g-jitter on the mixed convection flow of Jeffrey fluid and micropolar nanofluids past an inclined stretching sheet with the presence of nanoparticles, while Hamdan et al. (2020) and Rosaidi et al. (2022) conducted their research based on free convection flow fluid since it is simpler to analyses the behaviors of the magnetic nanofluids because it naturally happens without affected by any external forces. Heat transfer analysis with convective boundary conditions is evoked in processes including high temperatures such as thermal energy storage, gas turbines, and nuclear plants (Akbar et al., 2013; Nadeem et al., 2013). There are several studies focused on the effect of a convective boundary condition on boundary layer flow and heat transfer over a stretching or shrinking surface of nanofluid (Alsaedi et al., 2012; Makinde and Aziz, 2011; Yao et al., 2011; Ghazali et al., 2021). Recently, Kanafiah et al. (2022) focused on the problem of steady combined convective transport by considering an alternative development of heat transfer fluids to solve the performance of the heat transfer process in industrial sectors.

However, to the extent of the authors' knowledge, attempts are yet to be made to address the issues of aligned MHD free convection heat transfer flow regarding magnetic nanofluids over a moving inclined plate with convective boundary condition. Hence, a study was conducted in an attempt to understand free convection boundary layer flow over a moving inclined plate for two magnetic nanofluids, namely Fe_3O_4-water and Fe_3O_4-kerosene.

2. Mathematical formulation

Consider the hydromagnetic free convection flow of magnetic nanofluid to be steady, incompressible, two-dimensional, and laminar over a moving inclined plate with the aligned and transverse magnetic field**.** The semi-infinite plate is inclined at an acute angle γ to the vertical axis measured in the clockwise direction and situated in an otherwise quiescent ambient fluid at the temperature T_∞. U_∞ is the constant free stream velocity? The plate is moving with constant velocity $U_w(x) = \lambda U_\infty$ where $U_w(x)$the plate velocity is, λ is the plate velocity parameter. The physical coordinates (x, y) are chosen such that x-axis measured along the inclined plate and y-axis is normal to the surface of the plate. The plate is heated by convection through a hot fluid at the temperature T_f with heat transfer coefficient h_f. The gravitational acceleration **g** is acting downward. The physical configuration of the problem is shown in Fig. 1. Water and kerosene are used as the base fluids with magnetite (Fe_3O_4) as nanoparticles. The base fluids and nanoparticles are in thermal equilibrium and no slip occurs between them. The spherical shaped nanoparticles are considered. The viscous dissipation and radiation are neglected in the analysis.

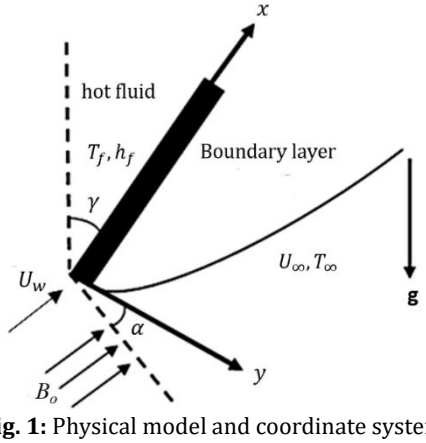

Fig. 1: Physical model and coordinate system

Under the above assumptions and following Tiwari and Das (2007), the equations of MHD boundary layer flow are:

$$\frac{\partial u}{\partial x}+\frac{\partial v}{\partial y}=0 \quad (1)$$

$$u\frac{\partial u}{\partial x}+v\frac{\partial u}{\partial y}=\frac{\mu_{nf}}{\rho_{nf}}\frac{\partial^2 u}{\partial y^2}+\frac{(\rho\beta)_{nf}}{\rho_{nf}}g\,cos\gamma(T-T_\infty)-\frac{\sigma B^2(x)}{\rho_{nf}}sin^2\alpha(u-U_\infty) \quad (2)$$

$$u\frac{\partial T}{\partial x}+v\frac{\partial T}{\partial y}=\alpha_{nf}\frac{\partial^2 T}{\partial y^2} \quad (3)$$

The boundary conditions for this problem are given by,

$$u=U_w(x)=\lambda U_\infty,\qquad v=0,\quad -k_{nf}\frac{\partial T}{\partial y}=h_f(T_f-T) \quad (4)$$

on

$$y=0$$
$$u\to U_\infty,\qquad T\to T_\infty,\text{ as } y\to\infty$$

where, u and v are the x (along the inclined plate) and y (normal to the plate) components of velocities, respectively. T is the temperature of the magnetic nanofluid, σ is the electrical conductivity and α is the aligned magnetic field angle. The transverse magnetic field assumed to be a function of the distance from the origin is defined as $B(x)=B_0x^{-\frac{1}{2}}$ with $B_0\neq 0$, where x is the coordinate along the plate and B_0 is the magnetic field strength. The effective properties of magnetic nanofluids may be expressed in terms of the properties of base fluids, nanoparticles, and the volume fraction of solid nanoparticles as follow (Khan et al., 2015).

$$\rho_{nf}=(1-\phi)\rho_f+\phi\rho_s,\quad \mu_{nf}=\frac{\mu_f}{(1-\phi)^{2.5}},\quad (\rho C_p)_{nf}=(1-\phi)(\rho C_p)_f+\phi(\rho C_p)_s,\quad (\rho\beta)_{nf}=(1-\phi)(\rho\beta)_f+\phi(\rho\beta)_s$$
$$\alpha_{nf}=\frac{k_{nf}}{(\rho C_p)_{nf}},\qquad \frac{k_{nf}}{k_f}=\frac{k_s+2k_f-2\phi(k_f-k_s)}{k_s+2k_f+\phi(k_f-k_s)} \quad (5)$$

where, ρ_{nf} is the effective density, ϕ is the solid volume fraction, ρ_f is the density of the pure base fluid, ρ_s is the density of nanoparticles, μ_f is the dynamic viscosity of the base fluids, μ_{nf} is the effective dynamic viscosity, $(\rho C_p)_{nf}$ is the heat capacity of the magnetic nanofluids, $(\rho C_p)_f$ is the specific heat parameters of the base fluids, $(\rho C_p)_s$ is the specific heat parameters of nanoparticles, $(\rho\beta)_{nf}$ is the thermal expansion coefficient, α_{nf} is the thermal diffusivity of the magnetic nanofluids, k_{nf} is the thermal conductivity of the magnetic base fluid, k_f is the thermal conductivity of the magnetic nanofluids and k_s is the thermal conductivity of nanoparticles. Continuity 1 is satisfied by introducing a stream function $\psi(x,y)$ below

$$u=\frac{\partial\psi}{\partial y},\quad v=-\frac{\partial\psi}{\partial x} \quad (6)$$

The following similarity variables are introduced:

$$\eta=y\sqrt{\frac{U_\infty}{v_f x}}=\frac{y}{x}\sqrt{Re_x}\ ,\ \psi=v_f\sqrt{Re_x}f(\eta)\ ,\ \theta(\eta)=\frac{T-T_\infty}{T_f-T_\infty} \quad (7)$$

where, η is the similarity variable, $Re_x=U_\infty x/v_f$ is the Reynolds number, $f(\eta)$ the non–dimensional stream function and $\theta(\eta)$ the non–dimensional temperature.

On the use of Eqs. 5–7, Eqs. 2–3 reduce to the following nonlinear system of ordinary differentials equations:

$$f'''+(1-\phi)^{2.5}\left(1-\phi+\phi\left(\frac{\rho_s}{\rho_f}\right)\right)\frac{1}{2}ff''+(1-\phi)^{2.5}M(1-f')sin^2\alpha+(1-\phi)^{2.5}\left(1-\phi+\phi\left(\frac{(\rho\beta)_s}{(\rho\beta)_f}\right)\right)Gr_x\theta cos\gamma=0 \quad (8)$$

$$\left(\frac{k_{nf}}{k_f}\right)\theta''+\frac{Pr}{2}\left(1-\phi+\phi\frac{(\rho C_p)_s}{(\rho C_p)_f}\right)f\theta'=0 \quad (9)$$

subjected to the boundary conditions of Eq. 4 which become,

$$f(0)=0,\quad f'(0)=\lambda,\quad \theta'(0)=-Bi_x(1-\theta(0)),\text{ at }\eta=0$$
$$f'(\eta)\to 1,\quad \theta(\eta)\to 0,\quad \text{as }\eta\to\infty \quad (10)$$

where, primes denote differentiation with respect to η, M is the magnetic parameters where $M=\sigma {B_0}^2/\rho U_\infty$, Gr_x is the local Grashof number, $Gr_x=g\beta_f(T_f-T_\infty)x/{U_\infty}^2$ and Pr is the Prantl number, $Pr=(\mu C_p)_f/k_f$. Note that λ denotes the direction of motion of the plate. Here $\lambda=0$ for the static plate, while $\lambda<0$ is for the plate and the fluid moving in the opposite direction and $\lambda>0$ indicates the plate and the fluid move in the same. To have a true similarity solution, the parameter Gr_x and Bi_x must be constant and independent of x. This condition will be satisfied if the thermal expansion coefficient β_f proportional to x^{-1}. Hence, assume of Makinde (2011), $\beta_f=ax^{-1}$ where a is a constant but has the appropriate dimension. Substituting $\beta_f=ax^{-1}$ into the parameter Gr_x will result $Gr=ag(T_f-T_\infty)/{U_\infty}^2$. For Bi_x, $h_f=bx^{-1/2}$ will gives $Bi_x=\frac{h_f}{k_{nf}}\sqrt{\frac{v_f}{U_\infty}}$. The quantities of engineering interest are the local skin–friction coefficient, C_f at the surface of the plate and the local Nusselt number, Nu_x which are defined as:

$$C_f=\frac{\tau_w}{\rho_f {U_\infty}^2}\ ,\ Nu_x=\frac{xq_w}{k_f(T_f-T_\infty)} \quad (11)$$

where, τ_w is the wall skin friction or shear stress at the plate and q_w is the heat flux from the plate, which is given by:

$$\tau_w=\mu_{nf}\left(\frac{\partial u}{\partial y}\right)_{y=0}\ ,\ q_w=-k_{nf}\left(\frac{\partial T}{\partial y}\right)_{y=0} \quad (12)$$

Substituting Eqs. 5-7 into Eq. 12 and using Eq. 11,

$$C_f(Re_x)^{\frac{1}{2}} = \frac{1}{(1-\phi)^{2.5}} f''(0), \quad \frac{Nu_x}{(Re_x)^{\frac{1}{2}}} = -\frac{k_{nf}}{k_f}\theta'(0) \qquad (13)$$

3. Numerical techniques

The nonlinear ordinary differential equations in Eqs. 8–9 subject to boundary conditions of Eq. 10 are solved using the Keller–Box method, a well-known explicit finite difference scheme. This method is described in detail by Cebeci and Bradshaw (2012) and is very suitable for solving large numbers of nonlinear coupled equations. The following four steps are involved with this method.

1. Reduce Eqs. 8-9 to the first order system.
2. Write the difference equations using central differences.
3. Linearize the obtained algebraic equations by Newton's method and arrange them in a matrix-vector form.
4. Solve the linear system of equations by using the block tridiagonal elimination method.

4. Results and discussion

In this section, the simulation results of different variations of flow parameters are presented and discussed. Thermophysical properties of water, kerosene and Fe_3O_4 is presented in Table 1. The numerical results of non-dimensional velocity and temperatures are shown in Figs. 2–7. The parameters used for simulation are $\alpha = 90^o$, $M = 1$, $\gamma = 45^O$, $Gr_x = 0.1$, $\phi = 0.05$ and $Bi_x = 0.1$, unless otherwise stated:

Table 1: Thermophysical properties of base fluids and nanoparticles (Mojumder et al., 2015; Sheikholeslami et al., 2015; Ilias et al., 2017)

Physical Properties	Water	Kerosene	Fe_3O_4
$\rho(kg/m^3)$	997.1	780	5200
$C_p(J/kgK)$	4179	2090	670
$k(W/mK)$	0.613	0.149	6
$\beta \times 10^{-5}(K^{-1})$	21	99	1.3
Pr	6.2	21	

To validate the accuracy of the numerical method, a direct comparison was made with the previously reported numerical results by Ramesh et al. (2016) for different values of the Biot number. Based on Table 2, the obtained results are observed to be in good agreement with the earlier findings.

Table 2: Comparison result of $\theta(0)$ for different values of the Biot number (Bi_x) when $M = 0$, $Pr = 0.72$, $Gr_x = 0.5$, $\phi = 0$ and $\frac{k_{nf}}{k_f} = 1$

Bi_x	Ramesh et al. (2016)	Present	Ramesh et al. (2016)	Present	Ramesh et al. (2016)	Present
	$\alpha = 90^o$		$\alpha = 30^o$		$\alpha = 0^o$	
0.05	0.1446	0.144660	0.1394	0.139477	0.1388	0.138810
0.1	0.2527	0.252756	0.2401	0.240119	0.2386	0.238622
0.2	0.4035	0.403520	0.3800	0.380015	0.3774	0.377434
0.4	0.5750	0.575012	0.5431	0.543185	0.5398	0.539854
0.6	0.6699	0.669914	0.6371	0.637147	0.6337	0.633763
0.8	0.7301	0.730168	0.6986	0.698690	0.6954	0.695454
1.0	0.7718	0.771821	0.7422	0.742245	0.7392	0.739209
5	0.9441	0.944173	0.9334	0.933433	0.9323	0.932320
10	0.9712	0.971285	0.9654	0.965434	0.9648	0.964825

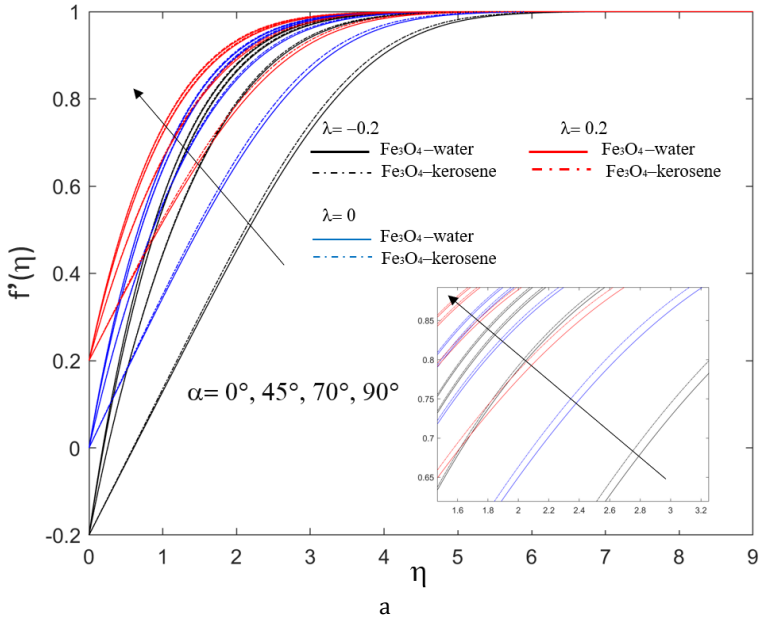

a

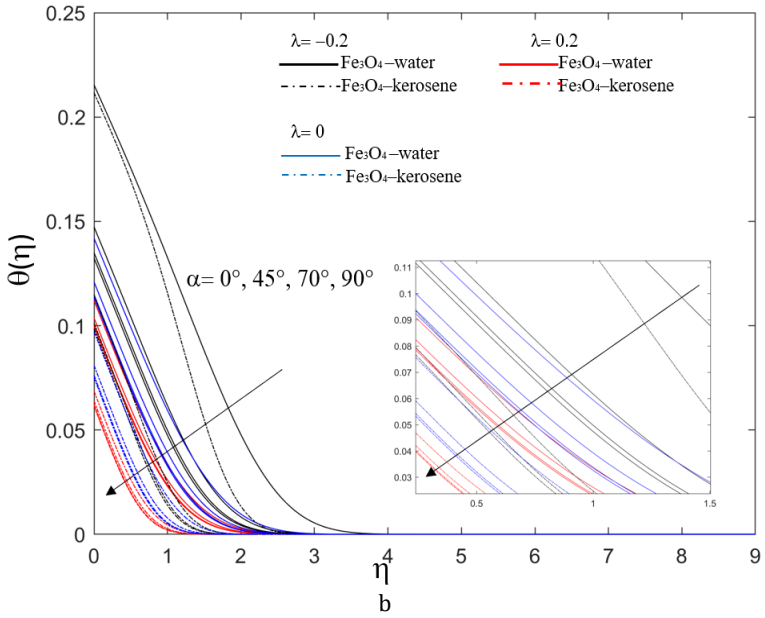

Fig. 2: Effect of aligned magnetic field angle parameter on the (a) velocity and (b) temperature profiles

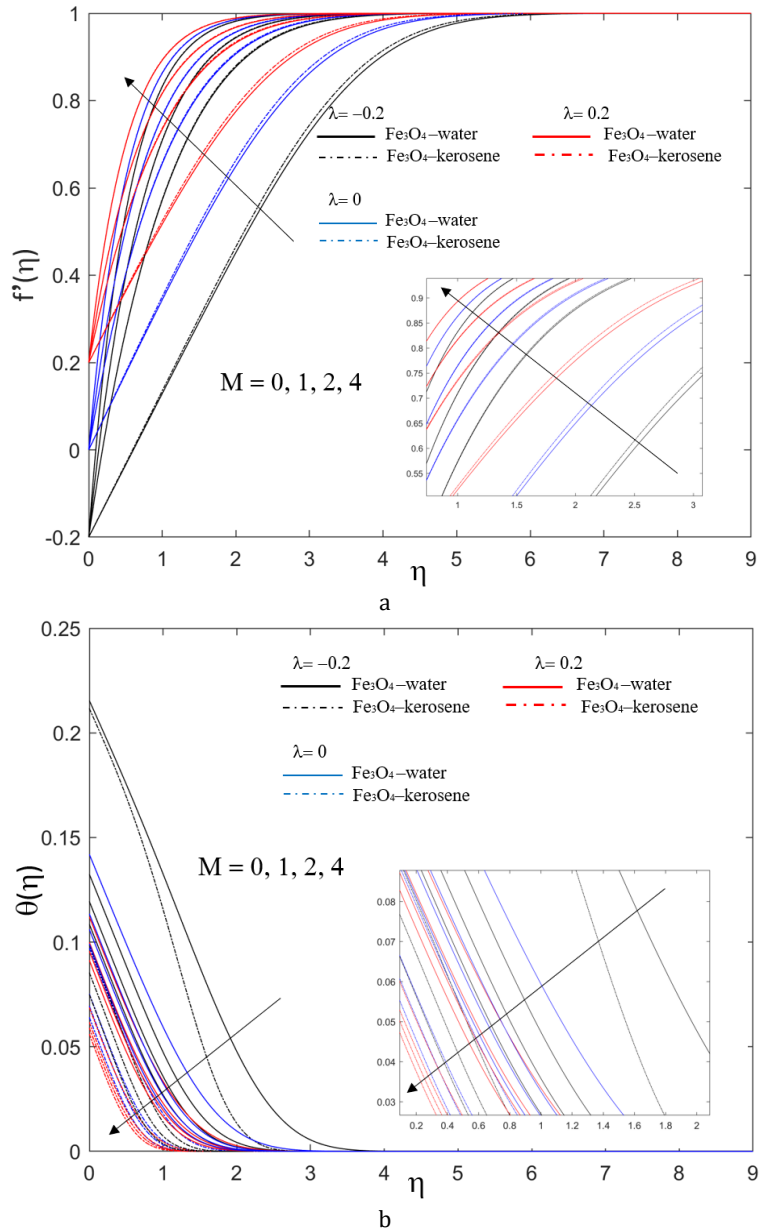

Fig. 3: Effect of magnetic strength parameter on the (a) velocity and (b) temperature profiles

As illustrated in Fig. 2, the influence of aligned magnetic field angle α, on velocity and temperature profiles of both Fe_3O_4-water and Fe_3O_4-kerosene magnetic nanofluids are observed. It is concluded that enhanced velocity profiles and reduced temperature profiles are achieved for both magnetic nanofluids with an increase in α. Further, a decline in the momentum boundary layer and the thermal boundary layer are seen with increasing α in the case of both magnetic nanofluids. This could be due to the strengthening of the applied magnetic field causing an increase in the value of the aligned angle ($0^o \leq \alpha \leq 90^o$) in the inclined plate. At $\alpha = 90^o$, this aligned magnetic field behaves like a transverse magnetic field and the magnetic field attracts nanoparticles because of the change in the aligned magnetic field's positions. For case $\lambda = 0.2$ the velocity profiles are high but the temperature is low compared to the other two cases ($\lambda = -0.2$ and $\lambda = 0$). As observed in Fig. 3, an increase in magnetic field parameter causes a monotonic rise in the fluid velocity profiles along with a decrease in temperature. Moreover, for both magnetic nanofluids, a decrease in momentum and thermal boundary layer can be seen. From Figs. 3a and 3b, Fe_3O_4-kerosene shows the highest velocity profiles and lowest temperature compared to Fe_3O_4-water.

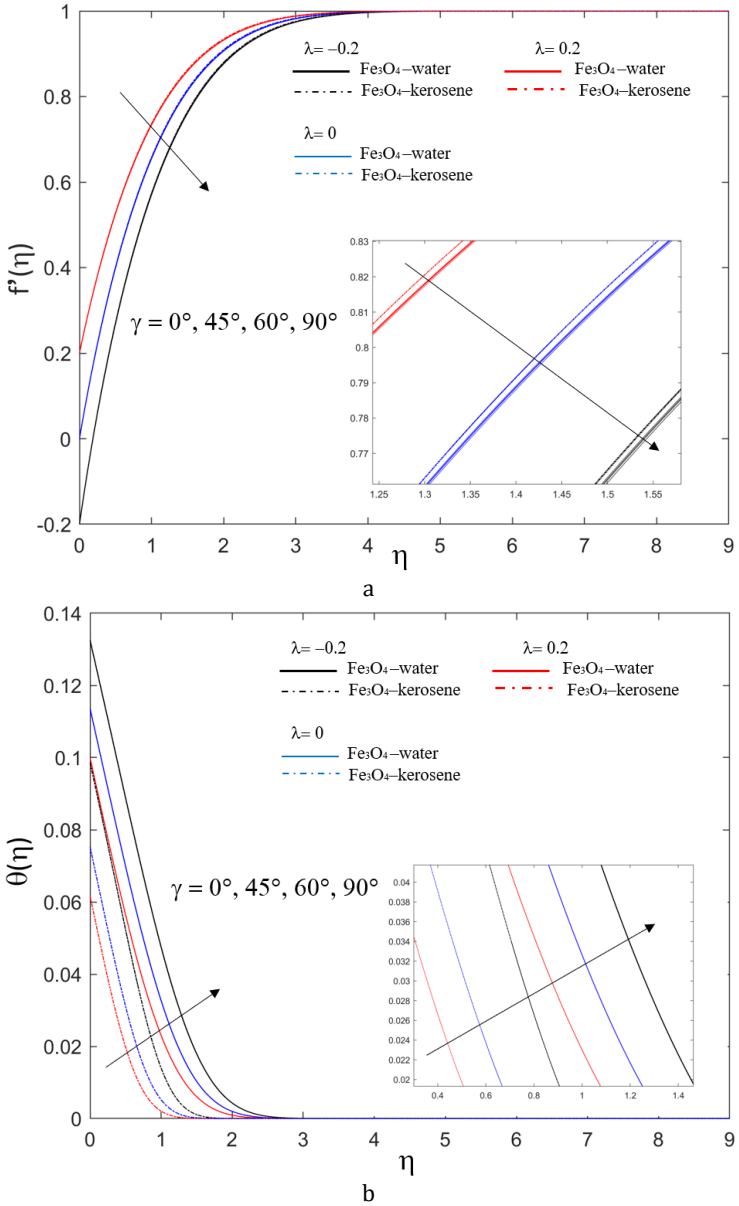

Fig. 4: Effect of inclined plate angle parameter on the (a) velocity and (b) temperature profiles

Fig. 4 shows a deceleration occurring in the velocity of magnetic nanofluids with an increase in the inclination of plate γ. The plate assumes a vertical position if $\gamma = 0^o$ while it is horizontal if $\gamma = 90^o$. For $\gamma = 90^o$, the gravitational effect is minimum while it is maximum for $\gamma = 0^o$. An increase of γ causes increase in the momentum and thermal boundary layer for both magnetic nanofluids. Fig. 5, shows that an increase in the Gr_x, the velocity are increases while the temperature profile decrease. As can be seen from Figs. 5a and 5b, the thicknesses of thermal and momentum boundary layers decrease with a rise in Gr_x due to the buoyancy effect. Positive values of local Grashof number $Gr_x > 0$ are

employed for the computations, which corresponds to the cooling issue with regards to the application. Most engineering applications often encounter cooling issue.

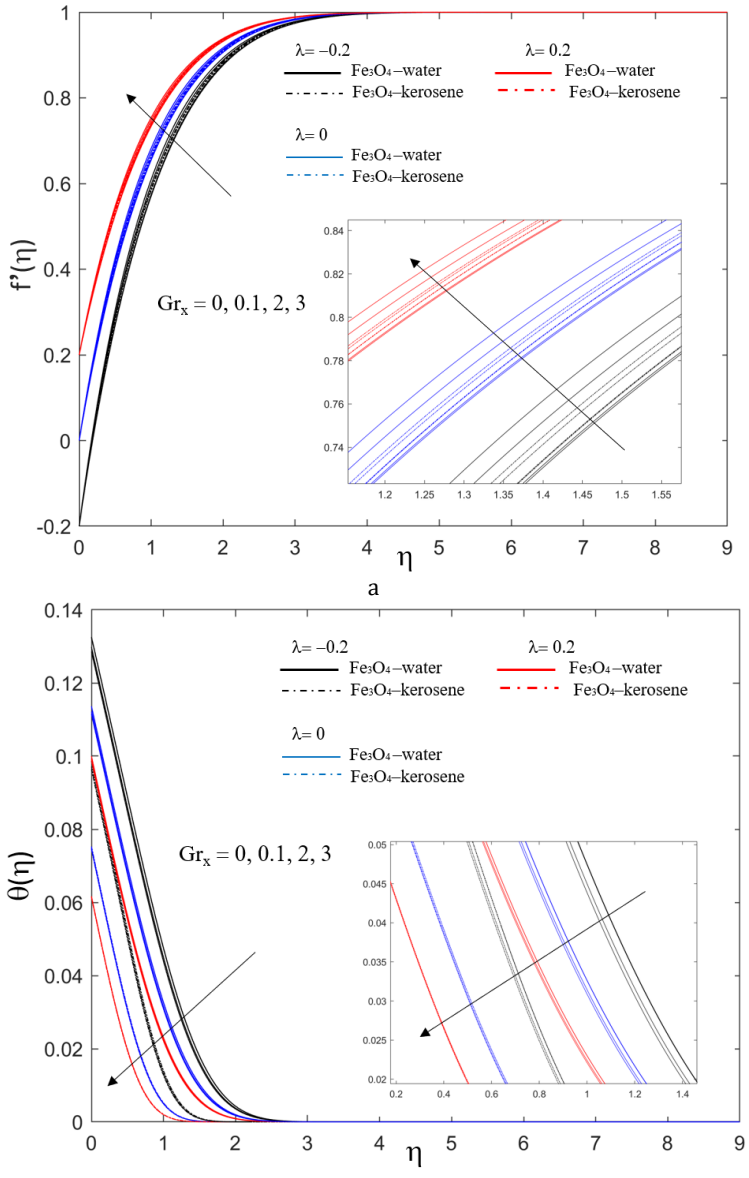

Fig. 5: Effect of local Grashof number on the (a) velocity and (b) temperature profiles

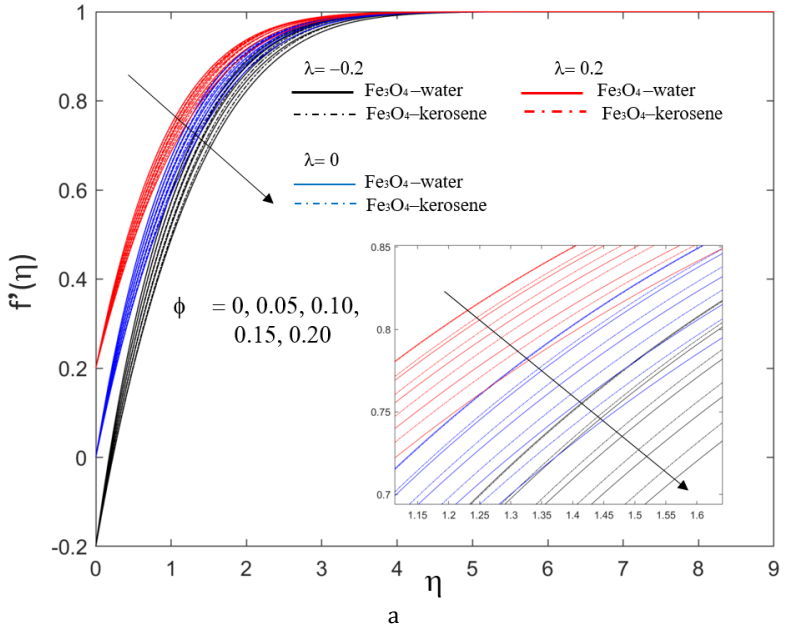

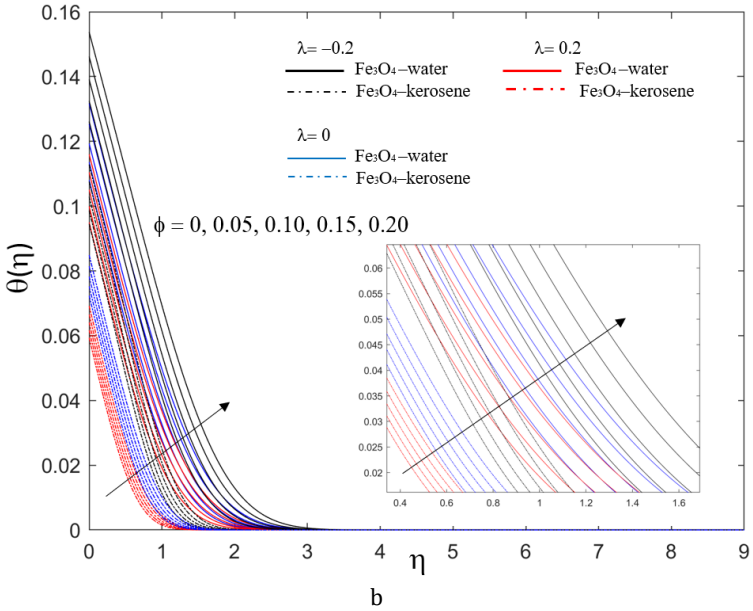

b

Fig. 6: Effect of volume fraction of nanoparticles on the (a) velocity and (b) temperature profiles

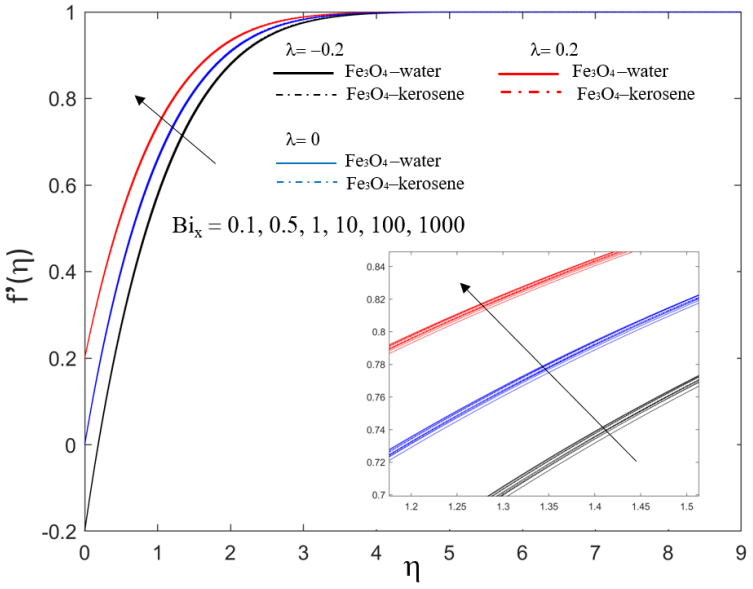

a

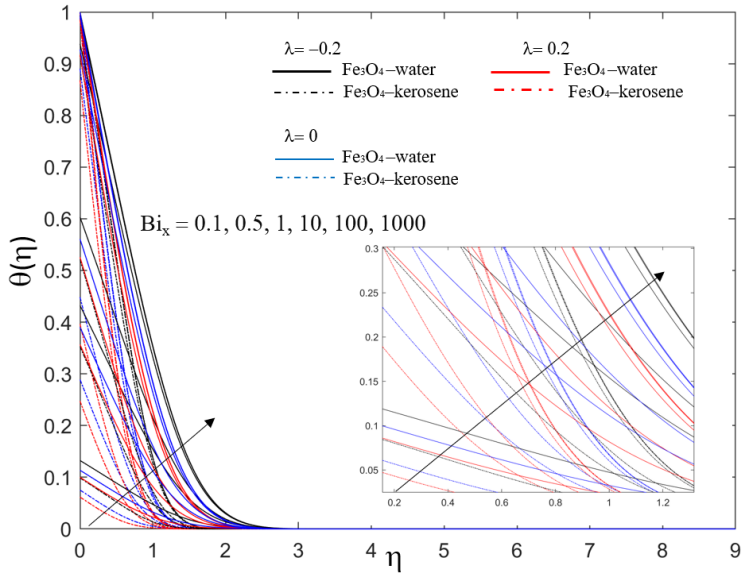

b

Fig. 7: Effect of convection parameter, Bi_x on the (a) velocity and (b) temperature profiles for different values of the plate velocity parameter (λ)

Fig. 6 presents the velocity and temperature profiles for different volume fraction values, ϕ. For both magnetic nanofluids, the velocity decreases with an increase in ϕ, while the momentum boundary layer increases. This is caused by the increase in the number of collisions amongst solid particles, which consequently results in the velocity reduction of magnetic nanofluids. For temperature distribution, temperature, as well as the thermal boundary layer thickness, are enhanced with an increase in solid ϕ. For the temperature profile, as the distance increases from the boundary, the distribution asymptotically moves toward zero. This is in agreement with the physical behavior that states an increase in thermal conductivity as well as thickness of the thermal boundary layer with the increase in the volume fraction of Fe_3O_4–kerosene and Fe_3O_4–water.

Fig. 7 illustrates the effect of the convection parameter, Bi_x on velocity and temperature profiles for both magnetic nanofluids at different values of moving inclined plate parameters, $\lambda = -0.2$, $\lambda = 0$, and $\lambda = 0.2$. It is seen from Figs. 7a and 7b that magnetic nanofluids' velocity increases with the increase of Bi_x, while the momentum boundary layer decreases. It can also be concluded that the temperature profiles and thermal boundary layer thickness increase with the increase of Bi_x. A similar observation has been reported by many reserachers (Ramesh et al., 2016; Sharma and Gupta, 2017; Dash and Mishra, 2022; Yesodha et al., 2022). As the value of the parameter Bi_x increases, the intensity of convective heating on the plate surface increases, which leads to an increasing rate of convective heat transfer from the hot fluid on the lower surface of the plate to the magnetic nanofluids on the upper surface. The graph also reveals that temperature increases rapidly near the surface due to the increasing values of Bi_x. Thermal boundary layer for Fe_3O_4-water is higher compared to Fe_3O_4-kerosene. For $\lambda = 0.2$, the velocity and temperatue profiles is higher compared to another two cases. For each curve, the vertical intercept gives the plate surface temperature. The plate surface temperature increases as Bi_x increases. As $Bi_x \to \infty$, the solution approaches the classical solution for the constant surface temperature. This can be seen from the boundary condition 10 which reduces to $\theta'(0) - Bi_x(1-\theta) \to \infty$ as $Bi_x \to \infty$.

Table 3 presents the variation occurring in skin friction coefficient for different $\alpha, M, \gamma, Gr_x, \phi$ and Bi_x values applicable to various inclined plate movements. For all three cases, it could be clearly seen that parameters ($\alpha, M, \gamma, Gr_x, \phi$ and Bi_x) had a boosting effect on the friction factor coefficients, especially for the case when $\lambda = -0.2$. The highest value could be seen for the case when M, Gr_x and ϕ are modified. It is interesting to note that in the case $\lambda = 0.2$, the friction factor coefficient was found to be lesser than in the cases of $\lambda = -0.2$ and $\lambda = 0$. So, the friction between the particles can be decreased in the case of $\lambda = 0.2$. In all cases, skin friction for Fe_3O_4-kerosene is higher than Fe_3O_4-water except for γ.

Table 4 lists the different variations in the Nusselt number for different values of dimensionless parameters. For all three cases, an enhancement was seen in the heat transfer rates with improving values of $\alpha, M, \gamma, Gr_x, \phi$ and Bi_x, especially for $\lambda = 0.2$ can be benefit to the heat transfer rates. The highest value could be seen for the case when ϕ and Bi_x in the case $\lambda = 0.2$. In all cases, Nusselt number for Fe_3O_4-kerosene is higher than Fe_3O_4-water except for γ.

Table 3: Variation in local skin friction for both magnetic nanofluids at different dimensionless parameters

α	M	γ	Gr_x	ϕ	Bi_x	Magnetic nanofluids (Fe_3O_4-water)			Magnetic nanofluids (Fe_3O_4-kerosene)		
						$\lambda = -0.2$	$\lambda = 0$	$\lambda = 0.2$	$\lambda = -0.2$	$\lambda = 0$	$\lambda = 0.2$
0^o						0.376803	0.397854	0.372688	0.383547	0.404891	0.380414
45^o						0.972052	0.841168	0.697534	0.973292	0.843750	0.700857
70^o	1	45^o	0.1	0.05	0.1	1.252000	1.066931	0.872440	1.252722	1.068702	0.874792
90^o						1.325944	1.127130	0.919493	1.326577	1.128750	0.921657
	0					0.376803	0.397854	0.372688	0.383547	0.404891	0.380414
	1					1.325944	1.127130	0.919493	1.326577	1.128750	0.921657
90^o	2	45^o	0.1	0.05	0.1	1.841523	1.550241	1.252808	1.841800	1.551207	1.254140
	4					2.581253	2.162081	1.738587	2.581357	2.162658	1.739403
		0^o				1.327898	1.128664	0.920739	1.327710	1.129485	0.922183
		45^o				1.325944	1.127130	0.919493	1.326577	1.128750	0.921657
90^o	1	60^o	0.1	0.05	0.1	1.324560	1.126044	0.918611	1.325775	1.128230	0.921286
		90^o				1.321214	1.123420	0.916481	1.323837	1.126973	0.920388
			0			1.321214	1.123420	0.916481	1.323837	1.126973	0.920388
			0.1			1.325944	1.127130	0.919493	1.326577	1.128750	0.921657
90^o	1	45^o	2	0.05	0.1	1.412744	1.196119	0.975921	1.377303	1.162133	0.945653
			3			1.456341	1.231363	1.005041	1.403068	1.179429	0.958183
				0		1.236444	1.047452	0.851737	1.234670	1.045716	0.850166
				0.05		1.325944	1.127130	0.919493	1.326577	1.128750	0.921657
90^o	1	45^o	0.1	0.1	0.1	1.426870	1.217024	0.995945	1.430301	1.222515	1.002384
				0.15		1.541411	1.319088	1.082754	1.548088	1.329037	1.094081
				0.2		1.672347	1.435805	1.182029	1.682795	1.450903	1.198965
					0.1	1.325944	1.127130	0.919493	1.326577	1.128750	0.921657
					0.5	1.336623	1.136148	0.927223	1.333635	1.133792	0.925477
90^o	1	45^o	0.1	0.05	1	1.342699	1.141712	0.932303	1.338297	1.137543	0.928544
					10	1.354573	1.153616	0.944052	1.349183	1.147937	0.938226
					100	1.356531	1.155723	0.946268	1.351255	1.150229	0.940632
					1000	1.356740	1.155950	0.946510	1.351481	1.150486	0.940909

Table 4: Variation in local Nusselt number for both magnetic nanofluids at different dimensionless parameters

α	M	γ	Gr_x	ϕ	Bi_x	Magnetic nanofluids (Fe_3O_4-water)			Magnetic nanofluids (Fe_3O_4-kerosene)		
						$\lambda=-0.2$	$\lambda=0$	$\lambda=0.2$	$\lambda=-0.2$	$\lambda=0$	$\lambda=0.2$
0^o						0.087569	0.095772	0.099109	0.090360	0.103473	0.106736
45^o						0.095167	0.098106	0.100032	0.101451	0.105329	0.107278
70^o	1	45^o	0.1	0.05	0.1	0.096549	0.098789	0.100380	0.103012	0.105870	0.107495
90^o						0.096834	0.098941	0.100462	0.103320	0.105991	0.107546
	0					0.087569	0.095772	0.099109	0.090360	0.103473	0.106736
	1					0.096834	0.098941	0.100462	0.103320	0.105991	0.107546
90^o	2	45^o	0.1	0.05	0.1	0.098285	0.099774	0.100938	0.104827	0.106652	0.107855
	4					0.099500	0.100547	0.101419	0.106022	0.107272	0.108182
		0^o				0.096841	0.098944	0.100464	0.103324	0.105992	0.107547
		45^o				0.096834	0.098941	0.100462	0.103320	0.105991	0.107546
90^o	1	60^o	0.1	0.05	0.1	0.096829	0.098939	0.100460	0.103318	0.105990	0.107546
		90^o				0.096817	0.098933	0.100457	0.103311	0.105988	0.107545
			0			0.096817	0.098933	0.100457	0.103311	0.105988	0.107545
			0.1			0.096834	0.098941	0.100462	0.103320	0.105991	0.107546
90^o	1	45^o	2	0.05	0.1	0.097128	0.099092	0.100546	0.103486	0.106042	0.107566
			3			0.097267	0.099167	0.100588	0.103567	0.106068	0.107577
				0		0.087391	0.089198	0.090504	0.090550	0.092764	0.094065
				0.05		0.096834	0.098941	0.100462	0.103320	0.105991	0.107546
90^o	1	45^o	0.1	0.1	0.1	0.106895	0.109352	0.111120	0.117277	0.120495	0.122352
				0.15		0.117634	0.120503	0.122560	0.132590	0.136473	0.138688
				0.2		0.129118	0.132475	0.134870	0.149466	0.154163	0.156808
					0.1	0.096834	0.098941	0.100462	0.103320	0.105991	0.107546
					0.5	0.316907	0.340425	0.359012	0.370852	0.407470	0.431387
					1	0.443003	0.490123	0.529456	0.548681	0.632448	0.691855
90^o	1	45^o	0.1	0.05	10	0.691267	0.812167	0.925370	0.967164	1.258666	1.516406
					100	0.732456	0.869440	1.000313	1.047349	1.397321	1.721888
					1000	0.736849	0.875617	1.008483	1.056111	1.412893	1.745549

5. Conclusions

A numerical study of the MHD free convection boundary layer flow for both water and kerosene magnetic nanofluids through an inclined plate subjected to a magnetic field has been analyzed. The following conclusions are derived.

1. The velocity increases with an increase of aligned magnetic field angle α, magnetic strength M, Grashof number Gr_x and Biot number Bi_x.
2. The velocity decreases with an increase of inclined plate angle γ and volume fractions of nanoparticles ϕ.
3. The temperature increases with an increase of inclined plate angle γ, volume fraction of nanoparticles ϕ, and Biot number Bi_x.
4. The temperature decreases with an increase of aligned magnetic field angle α, magnetic strength M and Grashof number Gr_x.
5. Skin friction coefficient and Nusselt number increase with the increase of aligned magnetic field angle α, magnetic strength M, Grashof number Gr_x, the volume fraction of nanoparticles ϕ and Biot number Bi_x for all three cases of inclined plate movements, $\lambda=-0.2$, $\lambda=0$, and $\lambda=0.2$.
6. Skin friction coefficient and Nusselt number decrease with the increase of inclined plate angle γ for all three cases of inclined plate movements, $\lambda=-0.2$, $\lambda=0$, and $\lambda=0.2$.

List of symbols

α	Aligned angle of magnetic field
α_{nf}	Thermal diffusivity of magnetic nanofluids
β_f	Thermal expansion coefficient
γ	Plate inclination angle
η	Boundary layer thickness
$\theta(\eta)$	Non – dimensional temperature function
λ	Velocity ratio parameter
μ_f	Dynamic viscosity of base fluid
μ_{nf}	Dynamic viscosity of magnetic nanofluids
ρ	Density
ρ_f	Density of base fluid
ρ_s	Density of nanoparticles
ρ_{nf}	Density of magnetic nanofluids
$(\rho C_p)_{nf}$	Heat capacity of magnetic nanofluids
$(\rho C_p)_f$	Heat parameters of base fluid
$(\rho C_p)_s$	Heat parameters of nanoparticles
$(\rho\beta)_{nf}$	Thermal expansion of magnetic nanofluids coefficient
σ	Electrical conductivity
τ_w	Wall shear stress
ϕ	Nanoparticles volume fraction
$\psi(x,y)$	Stream function
$B(x)$	Transverse magnetic field
B_0	Magnetic field strength
Bi_x	Biot number
$f(\eta)$	Non – dimensional stream function
C_f	Local skin – friction coefficient
Gr_x	Local Grashof number
g	Gravitational acceleration
h_f	Heat transfer coefficient
k_f	Thermal conductivity of base fluid
k_s	Thermal conductivity of nanoparticles.
k_{nf}	Thermal conductivity of magnetic nanofluids
M	Magnetic strength parameter
Nu_x	Local Nusselt number
Pr	Prantl number
q_w	Heat flux
Re_x	Reynolds number
T	Temperature
T_f	Temperature of hot fluid
T_∞	Temperature at the free stream
$U_w(x)$	Plate velocity
U_∞	Velocity in free stream
u	Velocity in x-direction

v Velocity in y-direction
x Dimensionless coordinate axis along the inclined plate
y Dimensionless coordinate axis normal to the surface plate

Acknowledgment

The authors extend their appreciation to Universiti Teknologi MARA Cawangan Kedah for funding this work through Geran Dana Kecemerlangan under grant number 600-UiTMKDH (PJI.5/4/1) (9/2018).

Compliance with ethical standards

Conflict of interest

The author(s) declared no potential conflicts of interest with respect to the research, authorship, and/or publication of this article.

References

Ahmad SZAS, Hamzah WAW, Ilias MR, Shafie S, and Najafi G (2019). Unsteady MHD boundary layer flow and heat transfer of Ferrofluids over a horizontal flat plate with leading edge accretion. Journal of Advanced Research in Fluid Mechanics and Thermal Sciences, 59(2): 163-181.

Akbar NS, Nadeem S, Haq RU, and Khan ZH (2013). Radiation effects on MHD stagnation point flow of nano fluid towards a stretching surface with convective boundary condition. Chinese Journal of Aeronautics, 26(6): 1389-1397. https://doi.org/10.1016/j.cja.2013.10.008

Alsaedi A, Awais M, and Hayat T (2012). Effects of heat generation/absorption on stagnation point flow of nanofluid over a surface with convective boundary conditions. Communications in Nonlinear Science and Numerical Simulation, 17(11): 4210-4223. https://doi.org/10.1016/j.cnsns.2012.03.008

Anjali Devi SP and Suriyakumar P (2013). Numerical investigation of mixed convective hydromagnetic nonlinear nanofluid flow past an inclined plate. AIP Conference Proceedings, 1557(1): 281-285. https://doi.org/10.1063/1.4823920

Bosli F, Suhaimi AS, Ishak SS, Ilias MR, Rahim AHA, and Ahmad AM (2022). Investigation of nanoparticles shape effects on aligned MHD Casson Nanofluid flow and heat transfer with convective boundary condition. Journal of Advanced Research in Fluid Mechanics and Thermal Sciences, 91(1): 155-171. https://doi.org/10.37934/arfmts.91.1.155171

Cebeci T and Bradshaw P (2012). Physical and computational aspects of convective heat transfer. Springer Science and Business Media, Berlin, Germany.

Choi SU and Eastman JA (1995). Enhancing thermal conductivity of fluids with nanoparticles (No. ANL/MSD/CP-84938; CONF-951135-29). Argonne National Lab. (ANL), Argonne, USA.

Dash AK and Mishra SR (2022). Free convection of micropolar fluid over an infinite inclined moving porous plate. Journal of Applied and Computational Mechanics, 8(4): 1154-1162.

Ghazali NMS, Abd Aziz AS, Soid SK, Ilias MR, and Ali ZM (2021). Stagnation point flow in copper nanofluid over slippery cylinder with viscous dissipation. Journal of Physics: Conference Series, 1770(1): 012041. https://doi.org/10.1088/1742-6596/1770/1/012041

Hamdan FR, Kamal MHA, Rawi NA, Mohamad AQ, Ali A, Ilias MR, and Shafie S (2020). G-jitter free convection flow near a three-dimensional stagnation-point region with internal heat generation. Journal of Advanced Research in Fluid Mechanics and Thermal Sciences, 67(1): 119-135.

Hussein AM, Sharma KV, Bakar RA, and Kadirgama K (2014). A review of forced convection heat transfer enhancement and hydrodynamic characteristics of a nanofluid. Renewable and Sustainable Energy Reviews, 29: 734-743. https://doi.org/10.1016/j.rser.2013.08.014

Ilias MR, Ismail NSA, AbRaji NH, Rawi NA, and Shafie S (2020). Unsteady aligned MHD boundary layer flow and heat transfer of a magnetic nanofluids past an inclined plate. International Journal of Mechanical Engineering and Robotics Research, 9(2): 197-206. https://doi.org/10.18178/ijmerr.9.2.197-206

Ilias MR, Rawi NA, and Shafie S (2017). Steady aligned MHD free convection of ferrofluids flow over an inclined plate. Journal of Mechanical Engineering, 14(2): 1-15.

Ilias MR, Rawi NA, Raji NHA, and Shafie S (2018). Unsteady aligned MHD boundary layer flow and heat transfer of magnetic nanofluid past a vertical flat plate with leading edge accretion. ARPN Journal of Engineering and Applied Sciences, 13(1): 340-351.

Ismail NSA, Abd Aziz AS, Ilias MR, and Soid SK (2021). MHD boundary layer flow in double stratification medium. Journal of Physics: Conference Series, 1770: 012045. https://doi.org/10.1088/1742-6596/1770/1/012045

Kamal MHA, Rawi NA, Ilias MR, Ali A, and Shafie S (2019). Effect of thermal radiation on a three-dimensional stagnation point region in nanofluid under microgravity environment. Universal Journal of Mechanical Engineering, 7: 272-284. https://doi.org/10.13189/ujme.2019.070504

Kanafiah SFHM, Kasim ARM, Zokri SM, and Ilias MR (2022). Combined convective transport of brinkman-viscoelastic fluid across horizontal circular cylinder with convective boundary condition. Journal of Advanced Research in Fluid Mechanics and Thermal Sciences, 89(2): 15-24. https://doi.org/10.37934/arfmts.89.2.1524

Khan WA, Khan ZH, and Haq RU (2015). Flow and heat transfer of ferrofluids over a flat plate with uniform heat flux. The European Physical Journal Plus, 130: 86. https://doi.org/10.1140/epjp/i2015-15086-4

Makinde OD (2011). Similarity solution for natural convection from a moving vertical plate with internal heat generation and a convective boundary condition. Thermal Science, 15(suppl. 1): 137-143. https://doi.org/10.2298/TSCI11S1137M

Makinde OD and Aziz A (2011). Boundary layer flow of a nanofluid past a stretching sheet with a convective boundary condition. International Journal of Thermal Sciences, 50(7): 1326-1332. https://doi.org/10.1016/j.ijthermalsci.2011.02.019

Mitra A (2018). Computational modelling of boundary-layer flow of a nano fluid over a convective heated inclined plate. Journal of Mechanics of Continua and Mathematical Sciences, 13(2): 88-94. https://doi.org/10.26782/jmcms.2018.06.00006

Mohamad AQ, Khan I, Jiann LY, Khan A, Ilias MR, and Shafie S (2017). Magnetohydrodynamic conjugate flow of Casson fluid over a vertical plate embedded in a porous medium with arbitrary wall shear stress. Journal of Nanofluids, 6(1): 173-181. https://doi.org/10.1166/jon.2017.1294

Mojumder S, Saha S, Saha S, and Mamun MAH (2015). Effect of magnetic field on natural convection in a C-shaped cavity filled with ferrofluid. Procedia Engineering, 105: 96-104. https://doi.org/10.1016/j.proeng.2015.05.012

Nadeem S, Haq RU, and Akbar NS (2013). MHD three-dimensional boundary layer flow of Casson nanofluid past a linearly stretching sheet with convective boundary condition. IEEE Transactions on Nanotechnology, 13(1): 109-115. https://doi.org/10.1109/TNANO.2013.2293735

Nayan A, Fauzan NIFA, Ilias MR, Zakaria SF, and Aznam NHZ (2022). Aligned Magnetohydrodynamics (MHD) flow of hybrid nanofluid over a vertical plate through porous medium. Journal of Advanced Research in Fluid Mechanics and Thermal

Sciences, 92(1): 51-64. https://doi.org/10.37934/arfmts.92.1.5164

Noranuar WNIN, Mohamad AQ, Shafie S, Khan I, Ilias MR, and Jiann LY (2021b). Analysis of heat transfer in non-coaxial rotation of Newtonian carbon nanofluid flow with Magnetohydrodynamics and porosity effects. In: Pham P (Ed.), 21st century nanostructured materials: Physics, chemistry, classification, and emerging applications in industry, biomedicine, and agriculture: 93-113. Books on Demand, Norderstedt, Germany.

Noranuar WNIN, Mohamad AQ, Shafie S, Khan I, Jiann LY, and Ilias MR (2021a). Non-coaxial rotation flow of MHD Casson nanofluid carbon nanotubes past a moving disk with porosity effect. Ain Shams Engineering Journal, 12(4): 4099-4110. https://doi.org/10.1016/j.asej.2021.03.011

Ostrach S (1952). An analysis of laminar free-convection flow and heat transfer about a flat plate parallel to the direction of the generating body force. Technical Report, National Advisory Committee for Aeronautics, Cleveland, USA.

Philip J, Shima PD, and Raj B (2007). Enhancement of thermal conductivity in magnetite based nanofluid due to chainlike structures. Applied Physics Letters, 91(20): 203108. https://doi.org/10.1063/1.2812699

Ramesh GK, Chamkha AJ, and Gireesha BJ (2016). Boundary layer flow past an inclined stationary/moving flat plate with convective boundary condition. Afrika Matematika, 27(1): 87-95. https://doi.org/10.1007/s13370-015-0323-x

Rana P, Bhargava R, and Bég OA (2012). Numerical solution for mixed convection boundary layer flow of a nanofluid along an inclined plate embedded in a porous medium. Computers and Mathematics with Applications, 64(9): 2816-2832. https://doi.org/10.1016/j.camwa.2012.04.014

Rawi NA, Ilias MR, Isa ZM, and Shafie S (2016). G-jitter induced mixed convection flow and heat transfer of micropolar nanofluids flow over an inclined stretching sheet. AIP Conference Proceedings, 1775(1): 030020. https://doi.org/10.1063/1.4965140

Rawi NA, Ilias MR, Jiann LY, Isa ZM, and Shafie S (2018). The effect of copper nanoparticles on mixed convection flow of Jeffrey fluid induced by g-jitter. Journal of Nanofluids, 7(1): 156-162. https://doi.org/10.1166/jon.2018.1433

Reddy PS, Sreedevi P, and Chamkha AJ (2017). MHD boundary layer flow, heat and mass transfer analysis over a rotating disk through porous medium saturated by Cu-water and Ag-water nanofluid with chemical reaction. Powder Technology, 307: 46-55. https://doi.org/10.1016/j.powtec.2016.11.017

Rosaidi NA, Ab Raji NH, Ibrahim SNHA, and Ilias MR (2022). Aligned Magnetohydrodynamics free convection flow of magnetic nanofluid over a moving vertical plate with convective boundary condition. Journal of Advanced Research in Fluid Mechanics and Thermal Sciences, 93(2): 37-49. https://doi.org/10.37934/arfmts.93.2.3749

Sharma K and Gupta S (2017). Homotopy analysis solution to thermal radiation effects on MHD boundary layer flow and heat transfer towards an inclined plate with convective boundary conditions. International Journal of Applied and Computational Mathematics, 3(3): 2533-2552. https://doi.org/10.1007/s40819-016-0249-5

Sheikholeslami M and Ganji DD (2014). Ferrohydrodynamic and Magnetohydrodynamic effects on ferrofluid flow and convective heat transfer. Energy, 75: 400-410. https://doi.org/10.1016/j.energy.2014.07.089

Sheikholeslami M, Ganji DD, and Rashidi MM (2015). Ferrofluid flow and heat transfer in a semi annulus enclosure in the presence of magnetic source considering thermal radiation. Journal of the Taiwan Institute of Chemical Engineers, 47: 6-17. https://doi.org/10.1016/j.jtice.2014.09.026

Tiwari RK and Das MK (2007). Heat transfer augmentation in a two-sided lid-driven differentially heated square cavity utilizing nanofluids. International Journal of Heat and Mass Transfer, 50(9-10): 2002-2018. https://doi.org/10.1016/j.ijheatmasstransfer.2006.09.034

Ullah I, Shafie S, and Khan I (2017). Effects of slip condition and Newtonian heating on MHD flow of Casson fluid over a nonlinearly stretching sheet saturated in a porous medium. Journal of King Saud University-Science, 29(2): 250-259. https://doi.org/10.1016/j.jksus.2016.05.003

Wu JM and Zhao J (2013). A review of nanofluid heat transfer and critical heat flux enhancement-Research gap to engineering application. Progress in Nuclear Energy, 66: 13-24. https://doi.org/10.1016/j.pnucene.2013.03.009

Xuan Y and Li Q (2000). Heat transfer enhancement of nanofluids. International Journal of Heat and Fluid Flow, 21(1): 58-64. https://doi.org/10.1016/S0142-727X(99)00067-3

Yao S, Fang T, and Zhong Y (2011). Heat transfer of a generalized stretching/shrinking wall problem with convective boundary conditions. Communications in Nonlinear Science and Numerical Simulation, 16(2): 752-760. https://doi.org/10.1016/j.cnsns.2010.05.028

Yesodha P, Bhuvaneswari M, Sivasankaran S, and Saravanan K (2022). Nanofluid flow with activation energy and heat generation under slip boundary condition with convective heat and mass transfer. Materials Today: Proceedings, 59: 959-967. https://doi.org/10.1016/j.matpr.2022.02.133